6. Guha C, Mohan S, Roy-Chowdhury N, Roy-Chowdhury J. Cell culture and animal models of viral hepatitis Part I: hepatitis B. Lab Anim 2004; 33: 37.
7. Durantel D, Zoulim F. Going towards more relevant cell culture models to study the in vitro replication of serum-derived hepatitis C virus and virus/host cell interactions? J Hepatol 2007; 46: 1.
8. Tateno C, Yoshizane Y, Saitou N et al. Near-completely humanized liver in mice shows human-type metabolic responses to drugs. Am J Pathol 2004; 165: 901.
9. Yoshizato K, Tateno C. A human hepatocyte-bearing mouse: an animal model to predict drug metabolism and effectiveness in humans. PPAR Res 2009; 2009: 476217.
10. Yoshizato K, Tateno C. In vivo modeling of human liver for pharmacological study using humanized mouse. Expert Opin Drug Metab Toxicol 2009; 5: 1435.
11. Katoh M, Matsui T, Okamura H et al. Expression of human phase II enzymes in chimeric mice with humanized liver. Drug Metab Dispos 2005; 33: 1333.
12. Nishimura M, Yoshitsugu H, Yokoi T et al. Evaluation of mRNA expression of human drug-metabolizing enzymes and transporters in chimeric mouse with humanized liver. Xenobiotica 2005; 35: 877.
13. Tsuge M, Hiraga N, Takaishi H et al. Infection of human hepatocyte chimeric mouse with genetically engineered hepatitis B virus. Hepatology 1046; 2005: 42.
14. Dandri M, Burda MR, Török E et al. Repopulation of mouse liver with human hepatocytes and in vivo infection with hepatitis B virus. Hepatology 2001; 33: 981.
15. Suemizu H, Hasegawa M, Kawai K et al. Establishment of a humanized model of liver using NOD/Shi-scid IL2Rg (null) mice. Biochem Biophys Res Commun 2008; 377: 248.
16. Meuleman P, Libbrecht L, de Vos R et al. Morphological and biochemical characterization of a human liver in a uPA-SCID mouse chimera. Hepatology 2005; 41: 847.
17. Igarashi Y, Tateno C, Tanaka Y et al. Engraftment of human hepatocytes in the livers of rats reconstructed with bone marrow cells from an immunodeficient mouse. Xenotransplantation 2008; 15: 235.
18. Laconi E, Oren R, Mukhopadhyay DK et al. Long-term, near-total liver replacement by transplantation of isolated hepatocytes in rats treated with retrorsine. Am J Pathol 1998; 153: 319.
19. Katayama S, Tateno C, Asahara T, Yoshizato K. Size-dependent in vivo growth potential of adult rat hepatocytes. Am J Pathol 2001; 158: 97.
20. Mori M, Mori Y, Hotta D et al. Changes in the size of liver lobules during neonatal growth of rat liver. Kanzo 1982; 23: 575.
21. van Rooijen N, Sanders A. Liposome mediated depletion of macrophages: mechanism of action, preparation of liposomes and applications. J Immunol Methods 1994; 174: 83.
22. van den Brink MR, Hunt LE, Hiserodt JC. In vivo treatment with monoclonal antibody 3.2.3 selectively eliminates natural killer cells in rat. J Exp Med 1990; 171: 197.
23. Tateno C, Takai-Kajihara C, Yamasaki C, Sato H, Yoshizato K. Heterogeneity of growth potential of adult rat hepatocytes in vitro. Hepatology 2000; 31: 65.
24. Masumoto N, Tateno C, Tachibana A et al. GH enhances proliferation of human hepatocytes grafted into immunodeficient mice with damaged liver. J Endocrinol 2007; 194: 529.
25. Utoh R, Tateno C, Kataoka M et al. Hepatic hyperplasia associated with discordant xenogeneic parenchymal–nonparenchymal interactions in human hepatocyte-repopulated mice. Am J Pathol 2010; 177: 654.
26. Wu CH, Ouyang EC, Walton C et al. Human hepatocytes transplanted into genetically immunocompetent rats are susceptible to infection by hepatitis B virus in situ. J Viral Hepat 2001; 8: 111.
27. Ouyang EC, Wu CH, Walton C et al. Transplantation of human hepatocytes into tolerized genetically immunocompetent rats. World J Gastroenterol 2001; 7: 324.
28. Nishie M, Tateno C, Utoh R et al. Hepatocytes from fibrotic liver possess high growth potential in vivo. Cell Transplant 2009; 18: 665.
29. Oinonen T, Lindros KO. Zonation of hepatic cytochrome P-450 expression and regulation. Biochem J 1998; 329: 17.
30. Wu YM, Joseph B, Gupta S. Immunosuppression using the mTOR inhibition mechanism affects replacement of rat liver with transplanted cells. Hepatology 2006; 44: 410.
31. Emoto K, Tateno C, Hino H et al. Efficient in vivo xenogeneic retroviral vector-mediated gene transduction into human hepatocytes. Hum Gene Ther 2005; 16: 1168.
32. Pruitt SK, Baldwin WM III, Barth RN, Sanfilippo F. The effect of xenoreactive antibody and B cell depletion on hyperacute rejection of guinea pig-to-rat cardiac xenografts. Transplantation 1993; 56: 1318.
33. Soares M, Havaux X, Nisol F et al. Modulation of rat B cell differentiation in vivo by the administration of an anti-mu monoclonal antibody. J Immunol 1996; 156: 108.
34. Geissler I, Sawyer GJ, Dong X et al. The effect of anti-lymphocyte serum on subpopulations of blood and tissue leucocytes: possible supplementary mechanisms for suppression of rejection and the development of opportunistic infections. Transpl Int 2005; 18: 1366.
35. Mashimo T, Takizawa A, Voigt B et al. Generation of knockout rats with X-linked severe combined immunodeficiency (X-SCID) using zinc-finger nucleases. PLoS ONE 2010; 25: e8870.
36. Mattocks AR, White IN. Toxic effects and pyrrolic metabolites in the liver of young rats given the pyrrolizidine alkaloid retrorsine. Chem Biol Interact 1973; 6: 297.

Laboratory Investigation (2013) 93, 54–71

Morphological and microarray analyses of human hepatocytes from xenogeneic host livers

Chise Tateno[1,2,3], Fuyuki Miya[4], Kenjiro Wake[5,6], Miho Kataoka[3], Yuji Ishida[1,2], Chihiro Yamasaki[1], Ami Yanagi[1], Masakazu Kakuni[1], Eddie Wisse[7], Fons Verheyen[7], Kouji Inoue[8], Kota Sato[9], Atsushi Kudo[9], Shigeki Arii[9], Toshiyuki Itamoto[10], Toshimasa Asahara[2,10], Tatsuhiko Tsunoda[4] and Katsutoshi Yoshizato[1,2,3,11]

We previously produced mice with human hepatocyte (h-hep) chimeric livers by transplanting h-heps into albumin enhancer/promoter-driven urokinase-type plasminogen activator-transgenic severe combined immunodeficient (SCID) mice with liver disease. The chimeric livers were constructed with h-heps, mouse hepatocytes, and mouse hepatic sinusoidal cells (m-HSCs). Here, we investigated the morphological features of the chimeric livers and the h-hep gene expression profiles in the xenogeneic animal body. To do so, we performed immunohistochemistry, morphometric analyses, and electron microscopic observations on chimeric mouse livers, and used microarray analyses to compare gene expression patterns in hepatocytes derived from chimeric mouse hepatocytes (c-heps) and h-heps. Morphometric analysis revealed that the ratio of hepatocytes to m-HSCs in the chimeric mouse livers were twofold higher than those in the SCID mouse livers, corresponding to twin-cell plates in the chimeric mouse liver. The h-heps in the chimeric mouse did not show hypoxia even in the twin-cell plate structure, probably because of low oxygen consumption by the h-heps relative to the mouse hepatocytes (m-heps). Immunohistochemical and electron microscopic examinations revealed that the sinusoids in the chimeric mouse livers were normally constructed with h-heps and m-HSCs. However, a number of microvilli projected into the intercellular clefts on the lateral aspects of the hepatocytes, features typical of a growth phase. Microarray profiles indicated that ~82% of 16 605 probes were within a twofold range difference between h-heps and c-heps. Cluster and principal component analyses showed that the gene expression patterns of c-heps were extremely similar to those of h-heps. In conclusion, the chimeric mouse livers were normally reconstructed with h-heps and m-HSCs, and expressed most human genes at levels similar to those in human livers, although the chimeric livers showed morphological characteristics typical of growth.

Laboratory Investigation (2013) **93,** 54–71; doi:10.1038/labinvest.2012.158; published online 12 November 2012

KEYWORDS: human hepatocytes; microarray; ultrastructure; uPA/SCID mouse

The liver is a critical organ that can develop a number of serious diseases, including viral hepatitis, alcoholic liver disease, nonalcoholic liver disease, liver cirrhosis, and hepatocarcinoma. From a medical perspective, the liver is also consequential as it can metabolize drugs in the body. Because of differences in liver metabolic function between humans and experimental animals, the results in preclinical efficacy or safety studies using animals do not always apply to humans. On the other hand, although *in vitro* metabolism tests using human hepatocytes (h-heps) have been used to predict the metabolites of new drugs in humans, the results of these studies show limitations in predictivity.[1] For investigating the mechanism of human liver disease and facilitating the development of medicines with high efficacy and safety for

[1]PhoenixBio Co., Ltd., Higashihiroshima, Japan; [2]Hiroshima University Liver Research Project Center, Hiroshima, Japan; [3]Yoshizato Project, Hiroshima Prefectural Institute of Industrial Science and Technology, Cooperative Link of Unique Science and Technology for Economy Revitalization (CLUSTER), Higashihiroshima, Japan; [4]Laboratory for Medical Informatics, Center for Genomic Medicine, RIKEN, Yokohama, Japan; [5]Liver Research Unit, Minophagen Pharmaceutical, Tokyo, Japan; [6]Department of Anatomy, School of Dental Medicine, Tsurumi University, Yokohama, Japan; [7]ELMI unit, Department of Molecular Biology, University Maastricht, Maastricht, The Netherlands; [8]Institute of Electron Microscopy, School of Dental Medicine, Tsurumi University, Yokohama, Japan; [9]Department of Hepatobiliary-Pancreatic Surgery, Graduate School of Medicine, Tokyo Medical and Dental University, Tokyo, Japan; [10]Division of Frontier Medical Science, Department of Surgery, and Hiroshima University 21st Century COE Program for Advanced Radiation Casualty Medicine, Programs for Biomedical Research, Graduate School of Biomedical Sciences, Hiroshima University, Hiroshima, Japan and [11]Developmental Biology Laboratory and Hiroshima University 21st Century COE Program for Advanced Radiation Casualty Medicine, Department of Biological Science, Graduate School of Science, Hiroshima University, Higashihiroshima, Japan
Correspondence: Dr C Tateno, PhD, PhoenixBio Co., Ltd., 3-4-1 Kagamiyama, Higashihiroshima, Hiroshima 7390046, Japan.
E-mail: chise.mukaidani@phoenixbio.co.jp

Received 16 April 2012; revised 24 August 2012; accepted 27 September 2012

humans, humanized animal models are needed, because they represent an approach that can circumvent the limitations of these other methods.

In a previous study, we transplanted h-heps into albumin enhancer/promoter-driven urokinase-transgenic severe combined immunodeficient (uPA/SCID) mice to create h-hep-bearing (chimeric) mice. The host mouse hepatocytes (m-heps) in the livers of the chimeric mice were replaced with h-heps[2] to the degree indicated by the replacement index (RI), which is the occupancy ratio of the h-hep area to the total (human and mouse) area on histological sections. In some cases, the RI in the mice was as high as 96%.[2] The transplanted h-heps expressed mRNA for a variety of human drug-metabolizing enzymes and transporters, in a manner similar to that of the donor liver.[2–4] The chimeric mouse livers were constructed with h-heps, m-heps, and mouse hepatic sinusoidal cells [m-HSCs; mainly Kupffer cells, sinusoidal endothelial cells (SECs), and stellate cells]. Moreover, the hepatocytes cooperated with the m-HSCs in liver function,[5,6] with the h-heps proliferating and functioning under the influence of the xenogeneic m-HSCs. However, few studies have investigated the structure of chimeric mouse livers[7,8] or comprehensively analyzed their gene expression patterns.

The present study was undertaken to study the morphological, biochemical, and genetic similarities or differences between the livers of humans, chimeric mice, and control mice in order to verify whether chimeric mice can be considered to be a relevant model for biomedical experiments concerning the human liver.

MATERIALS AND METHODS

Animals and Transplantation of H-heps

This study was performed with the ethical approval of PhoenixBio, and the Hiroshima Prefectural Institute of Industrial Science and Technology Ethics Board. The uPA/SCID mice were produced as previously described.[2] All transplantation experiments used homozygotic uPA/SCID mice as hosts. Cryopreserved h-heps from a 9-month-old Caucasian boy (9MM) were purchased from In Vitro Technologies (Baltimore, MD, USA). Cryopreserved h-heps from a 5-year-old African-American boy (5YM), a 2-year-old Caucasian boy (2YM), a 4-year-old Caucasian girl (4YF), a 6-year-old African-American girl (6YF), and a 10-year old Caucasian girl (10YM) were purchased from BD Biosciences (San Jose, CA, USA). These h-heps were used as donor cells for chimeric mice.

For the transplantation study, 1 or 2 tubes of cryopreserved h-heps ($5–15 \times 10^6$ cells/vial) were thawed and transplanted into 10–50 uPA/SCID mice ($2.5–10.0 \times 10^5$ viable cells/mouse). The human albumin (hAlb) concentration in the blood samples was periodically measured using latex agglutination immunonephelometry (LX Reagent 'Eiken' Alb II; Eiken Chemical, Tokyo, Japan) to predict the RI of h-heps in mouse livers.[2] The hAlb concentration in mouse blood correlated well with the RI. Chimeric mice (Table 1) were selected from each transplantation study for immunohistochemistry and enzyme histochemistry, blood flow measurements, oxygen consumption studies, electron microscopic examination, blood biochemistry, microarray analysis, and real-time quantitative reverse transcription-PCR (real-time qRT-PCR) analysis.

Immunohistochemistry and Enzyme Histochemistry

Frozen sections were prepared from the livers of 5YM-, 9MM-, and 2YM-chimeric mice (Table 1a, nos. 1–6), SCID mice, and humans (Table 1b). The sections were fixed in –20 °C acetone for 5 min, and then incubated with anti-human cytokeratin (CK) 8/18 (h-hep marker protein), anti-mouse CK18 (m-hep marker protein), BM8 (a mouse macrophage-specific antigen), anti-mouse stabilin II (mouse liver endothelial marker protein),[9] anti-desmin (stellate cell marker protein), anti-type IV collagen, anti-ZO-1, anti-claudin-1, and anti-occludin antibodies (tight junction proteins) (Table 2). The primary antibodies were visualized with Alexa 488- or 594-conjugated donkey anti-mouse-IgG, goat anti-rat IgG, or donkey anti-rabbit IgG (Invitrogen, Carlsbad, CA, USA) as secondary antibodies. The samples were then stained with Hoechst 33258 for nuclear staining. Human CK8/18 antibodies reacted with h-heps, but not m-heps; mouse CK18, BM8, and stabilin II antibodies reacted with m-cells, but not h-cells. Other antibodies reacted with both m- and h-cells (Table 2). Dipeptidyl dipeptidase IV (DPPIV) enzyme histochemistry was performed on liver cryosections as previously shown.[10]

Morphometric Analysis of Liver Cells

Three 5YM-chimeric mice (Table 1a, nos. 1–3) and 3 SCID mice were used in this study. To identify hepatocytes, liver cryosections from chimeric and SCID mice were stained with human CK8/18 and mouse CK18 antibodies, respectively, as above. Frozen sections from both mice were stained with BM8, anti-mouse stabilin II, and desmin antibodies. The numbers of h-heps and m-heps in an arbitrary area were counted as human CK8/18- or mouse CK8-positive cells, respectively. The number of Kupffer cells, SECs, and stellate cells in an arbitrary area were counted as BM8-, mouse-stabilin II-, and desmin-positive cells, respectively. The number of h-heps or m-heps, mouse Kupffer cells, mouse SECs, and mouse stellate cells in a unit area were calculated, and the ratios of component cells in the chimeric and SCID mouse livers were expressed as circle graphs.

Hypoxyprobe-1 treatment

To determine whether h-heps in the chimeric mouse livers were hypoxic, uPA/SCID mice transplanted with h-heps (5YM) or m-heps were injected with 60 mg/kg body weight pimonidazole HCl from the Hypoxyprobe-1 kit (Hypoxyprobe, Burlington, MA, USA), at 3 and 2 weeks after transplantation, respectively. The livers were subsequently

Table 1 Human liver tissues and chimeric mice used in this study

(a) Chimeric mice

Donors	*n*	Animal number (sex)	Weeks after transplantation	hAlb in blood (mg/ml)	RI (%)[a]	Purpose
5YM	3	1 (M), 2 (M), 3 (F)	13–15	12.2–16.5	87–95	Morphometric analysis, immunohistochemistry
9MM	2	4 (M), 5 (F)	11	3.1, 7.4	53, 75	Immunohistochemistry, enzyme histochemistry
2YM	1	6 (F)	10	13.3	97	Immunohistochemistry
5YM	3	7–9 (M)	14	8.2–11.4	75–85	ICG treatment
5YM	3	10–12 (M)	10	8.5–9.6	76–80	Microcirculation
5YM	3	13 (M), 14 (M), 15 (F)	11–14	15.9–17.5	94–97	Oxygen consumption
4YF	2	16 (F), 17 (M)	10, 16	7.5, 7.2	75, 74	Transmission electron microscopy
10YM	2	18 (M), 19 (F)	8	4.1, 4.9	57, 63	Transmission electron microscopy
2YM	2	20 (M), 21 (F)	12, 15	5.6, 11.6	69, 90	Scanning electron microscopy
9MM	3	22–24 (F)	10–14	6.0–16.1	70–95	Microarray, real-time qRT-PCR
6YF	3	25 (F), 26 (F), 27 (M)	11–12	11.2–14.6	91–100	Microarray
5YM	5	28–32 (M)	13 ± 1	11.1 ± 2.4	81 ± 6	Blood chemistry
5YM	5	33–37 (F)	13 ± 2	8.0 ± 1.3	71 ± 5	Blood chemistry

(b) Human liver tissues

Donors	Age (years)	Sex	Purpose
25YF	25	F	Microarray, real-time qRT-PCR, Immunohistochemistry
28YM	28	M	Microarray, real-time qRT-PCR
57YM	57	M	Microarray, real-time qRT-PCR
61YF	61	F	Microarray, real-time qRT-PCR

Abbreviations: F, female; hAlb, human blood albumin; M, male; RI, replacement index.
[a]RI calculated with blood hAlb levels using the formula of the correlation curve for each donor cell.

Table 2 Antibodies for immunohistochemistry

Antibodies	Clone	Host	Specificity	Dilution	Supplier
hCK8/18	Monoclonal	Mouse	h	100	Cappel Laboratory, (Cochranville, PA, USA)
mCK18	Monoclonal	Mouse	m	1	Progen Biotechnik. (Heidelberg, Germany)
BM8	Monoclonal	Rat	m	1000	BMA Biomedicals, (Augst, Switzerland)
mStabilin II	Monoclonal	Rat	m	1000	Gift from Dr Miyajima, (Tokyo University, Japan)
Desmin	Polyclonal	Rabbit	h, m	500	SYNBIO (Heidelberg, Germany)
Type IV collagen	Polyclonal	Rabbit	h, m	500	LSL (Tokyo, Japan)
ZO-1	Polyclonal	Rabbit	h, m	50	Zymed Laboratories (South San Francisco, CA, USA)
Claudin-1	Polyclonal	Rabbit	h, m	50	Zymed Laboratories
Occludin	Polyclonal	Rabbit	h, m	100	Zymed Laboratories

Abbreviations: h, human specific; m, mouse specific.

harvested at 1 h after the injection. Chimeric mice (5YM, nos. 1–3) at 13–15 weeks after transplantation and 14-week-old SCID mice were also treated with pimonidazole HCl in the same manner. Acetone-fixed, frozen liver sections were treated with anti-pimonidazole adduct mouse monoclonal antibodies and biotin-conjugated anti-mouse IgG (Hypoxyprobe-1 kit) and diaminobenzidine according to the manufacture's protocol.

Blood flow measurements

Indo-cyanine green (ICG, MP Biomedicals, LLC) dissolved in distilled water was injected into 3 chimeric mice (5YM, nos. 7–9) and 3 SCID mice via the tail vein at 25 mg/kg body weight. Blood was collected at 0, 2, 3, 4, 5, 6, 9, 12, 24, and 60 min after the injection, and the ICG concentrations were measured in the sera by the microplate reader system Vmax (Molecular Device, Ontario, Canada). The blood flow was calculated by moment analysis.

The microcirculation of the livers in 3 chimeric (5YM, nos. 10–12) and 3 SCID mice was observed under anesthesia using intravital videomicroscopy, as described previously.[11] For analyzing sinusoidal blood flow, at least 3 different sinusoids per mouse were captured in the microscopic fields at 500 frames/s using high-speed progressive videomicroscopy (HAS-LI, DITECT, Tokyo, Japan). This system enables high-resolution (1920 × 1080) capture of real-time red blood cell flow in the sinusoid, with the hydrodynamics analyzed by the Flowsizer 2D software (DITECT).

Measurement of Oxygen Consumption in H-Heps and M-Heps

Chimeric mouse hepatocytes (c-heps) and m-heps were isolated by the collagenase perfusion method from three 5YM-chimeric mice (nos. 13–15) and three SCID mice, respectively, as below. Donor hepatocytes (5YM), c-heps, and m-heps (1.5×10^6 cells) were incubated in 5 ml of 10 mM glucose in Dulbecco's modified Eagle's medium with 10% fetal bovine serum at 37 °C. Oxygen concentrations were measured every 5 min until 20 min using a SG6-ELK Professional dissolved oxygen meter (Mettler-Toledo KK, Tokyo, Japan). The oxygen consumption rate was calculated based on the oxygen concentration at each time point.

Electron Microscopy

The 4YF- and 10YM-chimeric mouse livers (Table 1a, nos. 16–19) were harvested under anesthesia. The mouse livers were prefixed by perfusing 1.5% glutaraldehyde in 0.1 M cacodylate buffer (pH 7.4) through a portal vein at 4 °C for 40 s using a syringe. The livers were cut into 1-mm^3 blocks with a razor blade under the affluent solution in 2% glutaraldehyde/0.1 M cacodylate buffer (pH 7.4). Next, the sample blocks were postfixed with 1% OsO_4/0.1 M phosphate buffer (pH 7.4) for 1 h at 4 °C. After the blocks were washed with 0.1 M phosphate buffer (pH 7.4), they were dehydrated through an ethanol series and propylene oxide, and embedded in Epon.[12] Ultrathin sections were cut with a Reichert Ultracut ultramicrotome (Reichert Optikwork, Vienna, Austria), stained with lead and uranyl salts, and examined in a JEOL-100 CX TEM (Tokyo, Japan) operated at 80 kV.

For scanning electron microscopy (SEM), the livers of 2YM-chimeric mice (Table 1a, nos. 20 and 21) were perfused through a portal vein with filtered 1.5% glutaraldehyde under anesthesia, and then with 1% sucrose/0.067 M cacodylate buffer (pH 7.4) at room temperature for 5 min.[13] The livers were cut into 1 × 1 × 5 mm blocks with a razor blade under the fixative solution, and washed with 1% sucrose/0.067 M cacodylate buffer (pH 7.4). The blocks were postfixed with 1% OsO_4/0.1 M phosphate buffer (pH 7.4) for 1 h at 4 °C, and then washed with 0.1 M phosphate buffer (pH 7.4). They were dehydrated with an ethanol series. After being treated with 100% ethanol, the samples were immersed for 10 min in 100% hexamethyldisilazane (Sigma Chemical), and dried in a desiccator. The samples were then mounted on stubs and sputter-coated with 10 nm of gold. They were observed under an SEM (model XL30, Philips).

Isolation of H-Heps from Human and Chimeric Mouse Livers for Microarray and Real-Time qRT-PCR Analyses

Livers were obtained from 4 individuals: 2 men aged 28 and 57 years (28YM and 57YM, respectively) and 2 women aged 25 and 61 years (25YF and 61YF, respectively; Table 1b). The donors gave informed consent before surgery, according to the 1975 Declaration of Helsinki. The h-heps were isolated from these tissues, as previously reported,[2] and subjected to microarray and real-time qRT-PCR analyses (Table 1b). The c-heps were isolated from 9MM-chimeric mice (Table 1a, nos. 22–24) 10–14 weeks after transplantation and 6YF-chimeric mice (Table 1a, nos. 25–27) 11–12 weeks after transplantation. These animals had high (>70%) RI levels (Table 1a). The livers were disaggregated using the two-step collagenase perfusion method:[14] the livers were perfused for 20 min, and then centrifuged 3 times at 50 *g* for 2 min. The hepatocytes obtained as pellets from the c-heps were used for the microarray and real-time qRT-PCR analyses. The cells were frozen in liquid nitrogen and stored in a deep freezer until total RNA isolation.

Microarray Analysis

Microarray-based gene expression analysis was performed at the hepatocyte level using c-heps or h-heps as RNA sources. Four human individuals (25YF, 28YM, 57YM, and 61YF; Table 1b) and 6 chimeric mice (Table 1a, nos. 22–27) were used in the microarray assay.

Total RNA was isolated from each hepatocyte sample using TRIzol reagent (Invitrogen), treated with DNase (Qiagen), and purified using the RNase-Free DNase Set (Qiagen) and the RNeasy Mini Kit (Qiagen). The RNAs from c-heps or h-heps were applied to the microarray assay using GeneChip Human Genome U-133 Plus 2.0 Array (Affymetrix, Santa Clara, CA, USA) with 54 675 probe sets according to the manufacturer's instructions. The obtained mRNA expression profiles (c-heps, $n = 6$; h-heps, $n = 4$) are designated as the hepatocyte-level profiles in this study. The gene expression array data were normalized using the MAS5 algorithm (Affymetrix). The signal reliability of each probe was determined based on the MAS5 Call algorithm (Affymetrix), and each probe was assigned to 1 of 3 flags (P, present; M, marginal; and A, absent). For correcting bias between chips, quantile normalization[15] was applied to all array data using

R software. We deposited our array data to NCBI GEO (Gene Expression Omnibus, http://www.ncbi.nlm.nih.gov/geo/, GEO ID GSE33846, GSE18674).

For determining the similarity of c-heps and h-heps, the microarray data of c-heps, h-heps, and 22 human tissues (h-tissues) (liver, kidney, pancreas, cerebellum, cortex, fetal brain, spinal cord, bone marrow, heart, skeletal muscle, salivary gland, colon, stomach, small intestine, lung, uterus, prostate, thyroid, trachea, spleen, thymus, and testis) were analyzed using principle component analysis (PCA) for 46 336 probes that were assigned as positive (P flag) for at least one of the flags in any of c-heps, h-heps, or 22 h-tissues, including h-liver. PCA and cluster analysis were performed using GeneSpring GX 11.0 (Agilent Technologies) and R software.

Liver signature probes were selected as follows: 685 and 805 probes with expression levels twofold higher or lower in the h-liver than in all of the other 21 h-tissues were selected among the 54 675 probes as liver high signature probes (Supplementary Table 1) and liver low signature probes (data not shown), respectively. The results of Gene Ontology (GO) and pathway analysis indicated that the selected 685 probes represent liver-specific components (Supplementary Table 2). Cluster analysis was performed with the average linkage method and Euclidian distance using Cluster and TreeView.[16]

Determination of mRNA Expression Levels by Real-Time qRT-PCR Analysis

A total of 17 human genes (*IGF-1*, *SOCS2*, *NNMT*, *IGFLS*, *KLOTHO*, *P4AH1*, *SLC16A1*, *SRD5A1*, *SCD*, *FADS1*, *FADS2*, *FASN*, *DGAT2*, *ADPN*, *SREBP1c*, *FABP*, and *AKR1B10*) were selected based on a previous study.[17] That is, these genes were previously determined to be up- or down-regulated in chimeric mouse livers when chimeric mice were administered human growth hormone (hGH).[17] The mRNA expression levels of these genes were quantified by real-time qRT-PCR. The specimens used for the microarray analysis were used for the extraction of total RNA, which was performed as described above. cDNA was synthesized using 1 μg of RNA, PowerScript reverse transcriptase (Clontech, Mountain View, CA, USA), and oligo-dT primers (Invitrogen) according to the manufacturer's instructions, and then subjected to real-time qRT-PCR. Genes were amplified with a set of gene-specific primers[17] and SYBR Green PCR mix in a PRISM 7700 Sequence Detector (Applied Biosystems, Tokyo, Japan). We confirmed conditions consisted of an initial denaturation step at 95 °C for 10 min, followed by 40 cycles at 95 °C for 15 s, and 60 °C for 1 min. All data were calculated by the comparative threshold cycle (Ct) method as previously described.[18] Contamination by m-heps did not affect the RT-PCR determination of human gene expression because the expression level of each gene was normalized against the human glyceraldehyde 3-phosphate dehydrogenase (hGAPDH) gene.

Gene Enrichment Analysis

Gene and GO information was collected from NCBI build 37 (http://ncbi.nlm.nih.gov) and the GO (http://www.geneontology.org) sites, respectively. Pathway information was collected from KEGG (http://www.genome.jp/kegg) and the Ingenuity Pathways Analysis (IPA) software (Ingenuity Systems). The gene enrichment analysis was performed using only GO and the pathway group when at least two or more genes were assigned.

Biochemical Tests

Blood was collected from the inferior vena cava of 5 male and 5 female 5YM-chimeric mice (Table 1a, nos. 28–37), 5 male uPA/SCID mice, and 3 male SCID mice at the time of killing. The sera were used for the following biochemical tests: glutamic pyruvic transaminase (GPT), glutamic oxaloacetic transaminase (GOT), γ-glutamyltransferase (GGT), cholinesterase (CHE), blood urea nitrogen (BUN), total cholesterol (TCHO), high-density lipoprotein cholesterol (HDL-c), triglycerides (TGs), total bilirubin (TBIL), glucose (GLU), total albumin (ALB), and total protein (TP). These tests were conducted using a Fuji Drichem 3500 V serum analyzer (Fujifilm, Tokyo, Japan).

Statistical Analyses

Microarray data were evaluated by Welch's *t*-test (two-sided) and adjusted for multiple testing using the Benjamini–Hochberg (B–H) false discovery rate (FDR).[19] The gene enrichment analysis and the significance of overlap between two groups of transcripts were performed using Fisher's exact test, and the gene enrichment analysis was corrected with the B–H FDR.[19] Data obtained in blood chemistry were analyzed among groups by ANOVA. When the overall F-statistics were significant, significance was determined by Sheffe's test with significance level $\alpha = 0.05$.

RESULTS

Construction of Chimeric Mouse Livers with H-Heps and M-HSCs

Cryopreserved donor hepatocytes (5YM) were thawed and transplanted into 54 2–4-week-old uPA/SCID mice (2.5×10^5 cells/animal), and blood hAlb concentrations were monitored (Figure 1a). In all, 50 mice remained alive beyond 10 weeks of age. Of these, 1, 3, and 2 mice showed 1–3, 3–5, and 5–7 mg/ml hAlb blood concentrations, respectively, at 10 weeks of age. Also, 44 mice secreted >7 mg/ml hAlb into the blood, and 6 mice died after reaching 10 weeks of age (5–7 mg/ml, $n = 1$; >7 mg/ml hAlb, $n = 5$). Three mice showing >7 mg/ml hAlb were used for morphometric analysis (nos. 1–3, Figure 1b and c). Immunohistochemistry showed that the hepatocytes and the nuclei were smaller in the chimeric mice than in the SCID mice (Figure 2a and b), which were similar to the h-heps in a human body (data not shown). BM8-positive mouse Kupffer cells (Figure 2c and d), desmin-positive mouse stellate cells (Figure 2g and h), and

m-Stabilin II-positive m-SECs (Figure 2e and f) were uniformly distributed in both livers, but their densities were lower in the chimeric mice than in the SCID mice. Desmin-positive mouse stellate cells with cytoplasmic projections were closely associated with the m-SECs (data not shown).

The BM8-positive mouse Kupffer cells were smaller in the chimeric mice ($39.2 \pm 4.3\,\mu m^2$) than in the SCID mice ($50.6 \pm 4.0\,\mu m^2$; Figure 2c and d). Moreover, large BM8-positive cells were occasionally present near portal veins in the chimeric mice (data not shown).

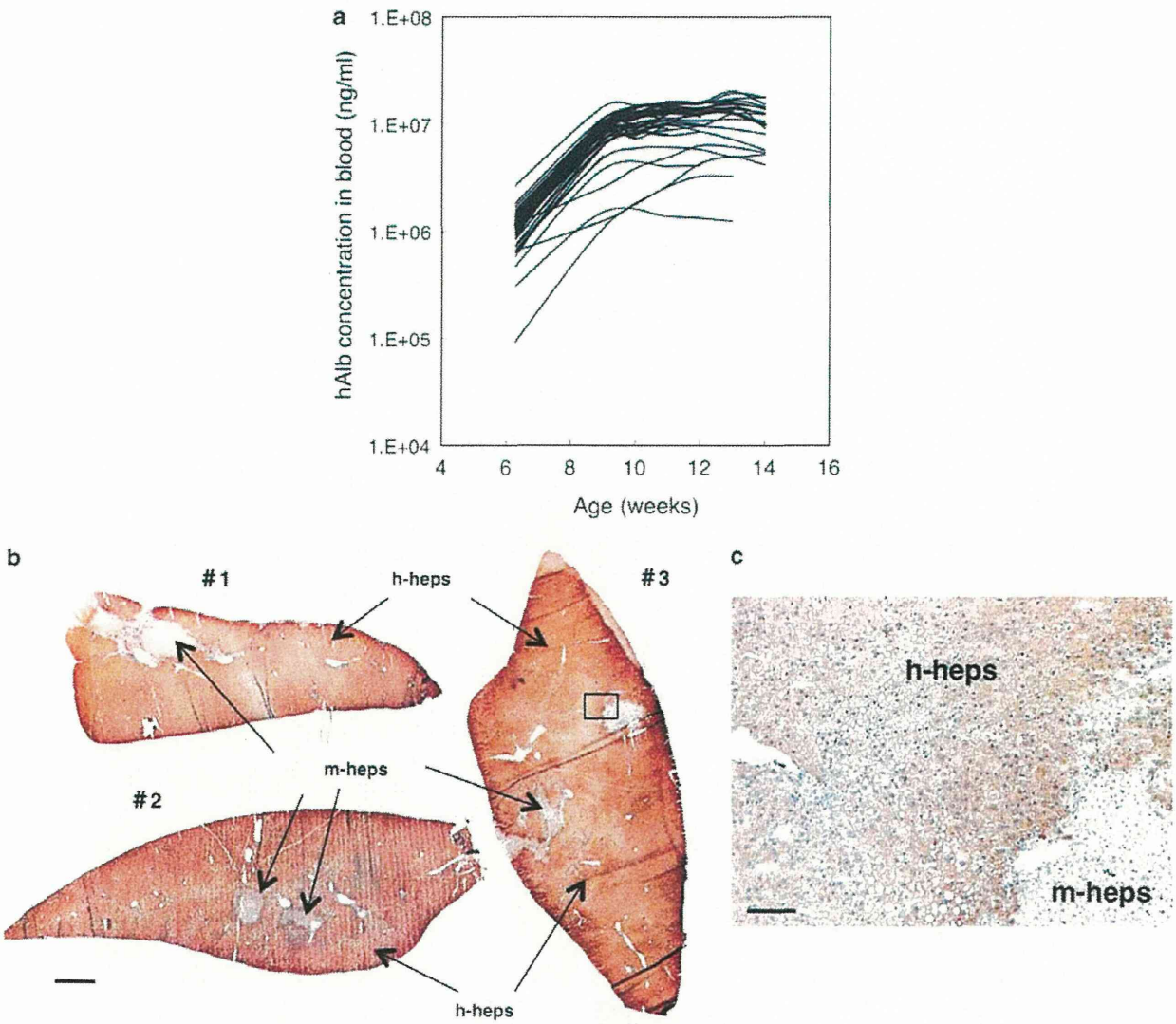

Figure 1 Changes in hAlb concentration in the blood and immunostained livers of mice transplanted with h-heps. (**a**) The graph shows an example of the results of the transplantation of h-heps into uPA/SCID mice. The h-heps from 5YM were transplanted into 54 uPA/SCID mice, and the hAlb concentrations in mouse blood were monitored. A total of 50 mice remained alive beyond 10 weeks of age. Of these, 1, 3, and 2 mice showed 1–3, 3–5, and 5–7 mg/ml hAlb concentrations, respectively, after 10 weeks of age. Forty-four mice leached >7 mg/ml hAlb into the blood, which corresponds to >70% RI. Three 5YM-chimeric mice were used for morphometric analysis. (**b**) The livers of three 5YM-chimeric mice (nos. 1–3) were immunostained with human CK8/18 antibodies. The brown-colored area is that of h-heps. The mouse livers were almost entirely repopulated by h-heps. Bar = 1 mm. (**c**) A magnified view of the liver region enclosed by the square for chimeric mouse no. 3 of (**b**). Bar = 100 μm.

Figure 2 Immunohistochemistry of SCID and chimeric mouse liver for morphometric analysis. Three SCID (**a**, **c**, **e**, **g**) and 5YM-chimeric mouse (**b**, **d**, **f**, **h**) livers were stained with Hoechst 33248 and m-CK18 (**a**) or h-CK8/18 (**b**); BM8 (**c**, **d**); anti-mouse stabilin II (**e**, **f**); desmin and m-CK18 (**g**) or h-CK8/18 (**h**). The cells and nuclei in the SCID mice were larger than those in the chimeric mice (**a**, **b**). The densities of BM8-, anti-mouse stabilin II-, and desmin-positive cells were lower in the chimeric mice than those in the SCID mice (**c**–**h**). BM8-positive cells were smaller in the chimeric mice than those in the SCID mice (**c**, **d**). Magnification is identical for panels belonging to the same horizontal pair. Bar = 100 μm.

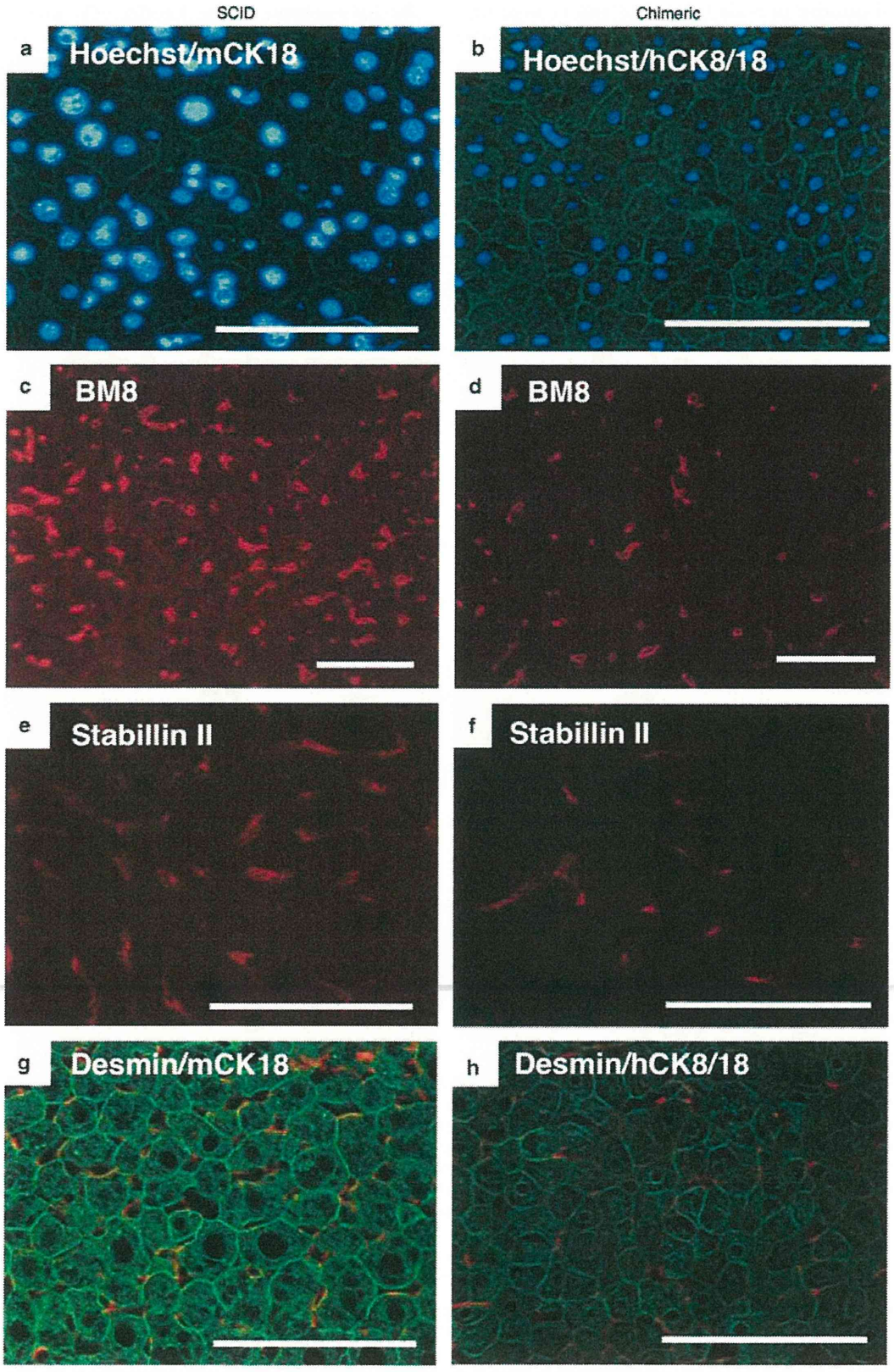

Figure 2 For caption please refer page 59.

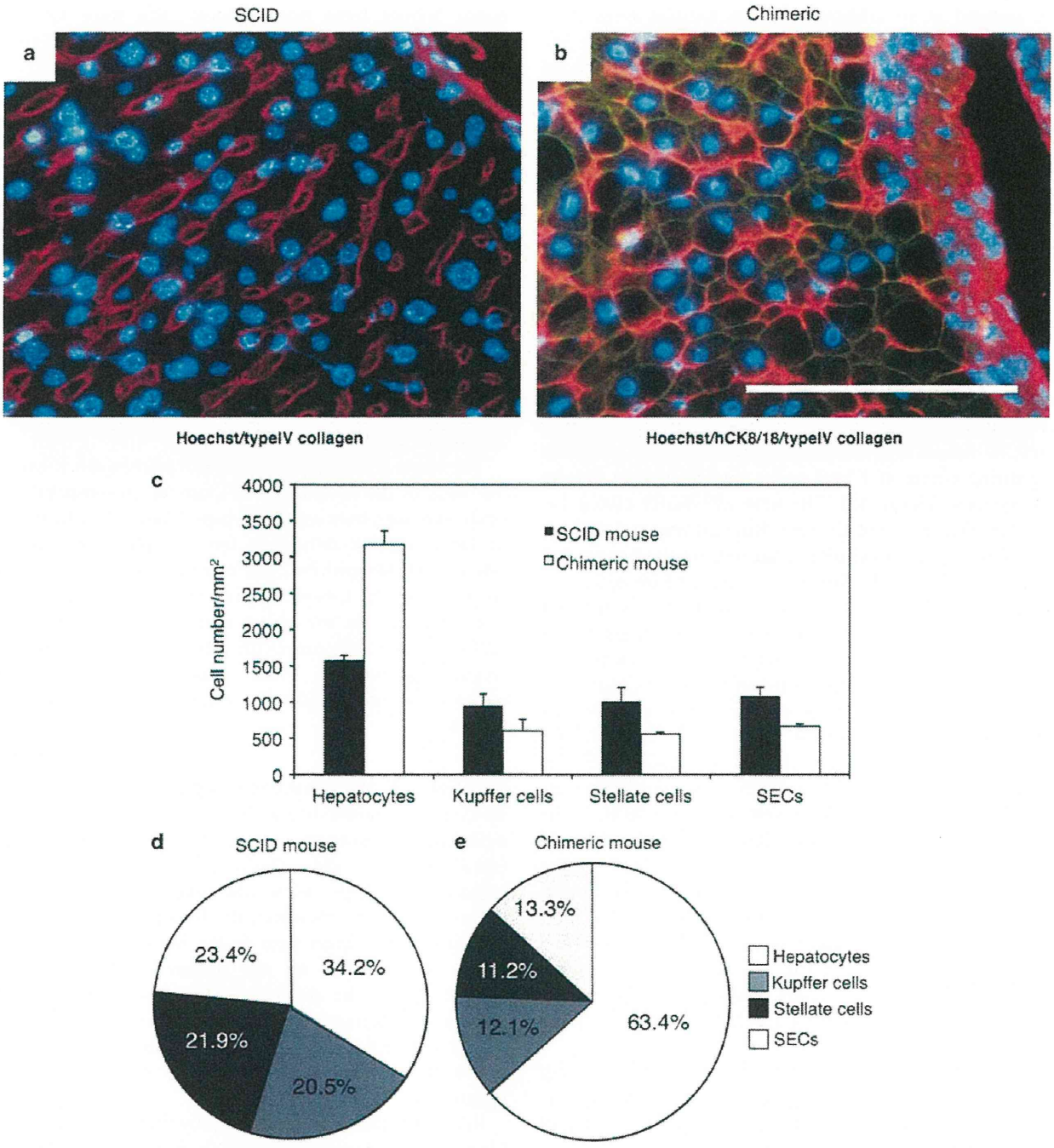

Figure 3 Immunohistochemistry of chimeric mouse livers stained for Type IV collagen, and the ratio of component cells in SCID (**a**) and chimeric (**b**) mouse livers. SCID and 5YM-chimeric mouse livers were stained with Hoechst and anti-type IV collagen antibody. 5YM-chimeric mouse livers were additionally stained with human CK8/18 antibodies. SCID and chimeric mouse livers showed single-cell and twin-cell plates, respectively. Bar = 100 μm. The number of hep cells, BM8-positive cells (Kupffer cells), desmin-positive cells (stellate cells), and anti-mouse stabilin II-positive cells (SECs) were counted under a microscope, and the density of each cell type was calculated (**c**). The ratios of the component cells in SCID (**d**) and chimeric mice (**e**) were calculated from the data of (**c**), and expressed as circle graphs. The ratios of Kupffer cells, stellate cells, and SECs were similar in the SCID and chimeric mice, but the ratio of hepatocytes to HSCs (Kupffer cells, stellate cells, and SEC) was twofold greater in the chimeric mice than that in the SCID mice.

Type IV collagen depositions were observed on the basal aspect of the heps (Figure 3a and b). In the SCID mouse liver, the m-heps showed single-cell plates (Figure 3a), whereas the h-heps in the chimeric mouse liver showed twin-cell plates (Figure 3b). The h-heps or m-heps in combination with the m-HSCs (m-Kupffer cells, m-SECs, and m-stellate cells)

were counted in an arbitrary area on samples from three chimeric mice or three SCID mice, respectively (Figure 3c), and the ratios were subsequently compared (Figure 3d and e). The ratios of the Kupffer cells, SECs, and stellate cells were similar between groups. However, the ratios of the h-heps and m-HSCs in the chimeric mice were twofold greater than those in the SCID mice (Figure 3d and e).

Lack of Hypoxia in H-Heps with Twin-Cell Plates

To determine whether the h-heps with the twin-cell plates were in a hypoxic state, the chimeric mice were treated with hypoxyprobe-1. The result revealed that the m-heps in the 14-week-old SCID mouse liver (Figure 4a) and the h-heps in the chimeric mouse liver at 13–15 weeks after transplantation (growth termination phase, Figure 4b) did not show hypoxia. The growing m-heps at 2 weeks after transplantation in the uPA/SCID mouse liver showed hypoxia (Figure 4c), whereas the growing h-heps at 3 weeks after transplantation did not show hypoxia (Figure 4d). The host uPA/SCID mouse hepatocytes (Figure 4c and d) were damaged and atrophic because of the expression of uPA. Thus, our results suggest that the damaged uPA/SCID mouse liver might be hypoxic.

As determined by measuring ICG concentrations, the liver blood flow was similar between the SCID and chimeric mice (Figure 4e and f), suggesting that the overall blood flow within the liver was similar between these two groups of mice. The livers of the chimeric mice were enlarged, with the liver weight to body weight ratio at $13.0 \pm 0.3\%$ for the chimeric mice and at $5.4 \pm 0.5\%$ for the SCID mice.[20] The microcirculation of the SCID and chimeric mice livers were then determined in order to investigate the effects of the enlarged liver size on sinusoidal blood flow in the chimeric mouse liver. The blood cell flow rate was slower in the sinusoids of the chimeric mouse liver ($0.0116 \pm 0.003\ \mu m/\mu s$, Figure 4g) than in those of the SCID mouse liver ($0.0247 \pm 0.005\ \mu m/\mu s$, Figure 4g). In addition, no disturbances were observed in the microcirculation of either the SCID or chimeric mice livers, despite the blood flow in the chimeric mouse liver occurring at half the rate seen in the SCID mouse liver.

The oxygen consumption of the c-heps increased in a cell number-dependent manner (Figure 4h). Moreover, the oxygen consumption of 1.5×10^6 m-heps was higher than that of 5.0×10^6 c-heps (Figure 4h). The oxygen consumption rates of m-heps from SCID mice, h-heps from chimeric mice, and donor h-heps from the chimeric mice were 4.82 ± 0.25, 1.07 ± 0.13, and $0.54\ \mu M/ml/10^6$ cells, respectively (Figure 4i).

Ultrastructure of Chimeric Mouse Livers

The chimeric mouse livers were found to be composed of three visually identifiable regions of different colors.[1] The white and red regions corresponded to the original diseased m-heps and uPA gene-deleted m-hep regions, respectively. The medium-toned regions between the white and red regions corresponded to h-heps. Electron microscopic observation showed that the h-heps in the medium-colored regions were distinguished as cells with abundant glycogen and large lipid droplets in the cytoplasm (Figure 5a). In contrast, abundant small granules (0.1–0.5 μm in diameter) were observed in the original diseased m-hep cells in the white regions (Figure 5b). M-heps in the red regions showed a normal morphology (Figure 5c).

The space of Disse was observed between the h-heps and the SECs of the mouse liver (Figure 5a), whereas bile canaliculi were seen between the h-heps (Figure 5d). In the space of Disse, stellate cells with lipid droplets were observed (Figure 5e). Meanwhile, SEM revealed fenestrae in the SECs (Figure 5f). The h-heps adhered to each other and formed bile canaliculi on the apical surfaces, whereas their basal surfaces had many microvilli facing the thin mouse SECs (Figure 5a and d). These results indicate normal reconstruction of the chimeric mouse livers with h-heps and m-HSCs.

Cell–Cell Adhesion Between Hepatocytes

In chimeric mouse livers, immunocytochemistry detected tight junction proteins, such as ZO-1 (Figure 6a), claudin-1 (data not shown), and occludin-1 (Figure 6c), on membranes adjacent to h-heps, as would occur in the human liver (Figure 6b and d). However, the frequency was lower in the chimeric mouse livers than in the human ones. DPPIV activity was observed on the microvilli of bile canaliculi (Figure 6f). In the chimeric mouse livers, DPPIV enzyme activity was concentrated on membranes adjacent to the h-heps. Interestingly, faint signals were detected on the h-hep cell surfaces near portal veins in the chimeric livers (Figure 6e).

Bile canaliculi are organized by junctional complexes. Electron microscopic examination demonstrated that junctional complexes, consisting of tight junctions, adherence

Figure 4 Analyses of pimonidazole binding (**a–d**), blood flow (**e–g**), and oxygen consumption (**h**, **i**) in SCID and chimeric mouse livers. SCID and chimeric mice and uPA/SCID mice transplanted with m-heps (2 weeks after transplantation) and h-heps (3 weeks after transplantation) were injected with pimonidazole HCl; the livers were then immunostained for pimonidazole adducts. SCID (**a**) and chimeric mouse livers (**b**) were negative for the adducts, whereas uPA/SCID mouse hepatocytes were positive for pimonidazole adducts (**c**, **d**). M-hep-colonies (**c**, arrowheads) were positive, whereas h-hep-colonies were negative (**d**, arrowheads). Bar = 100 μm. The chimeric mice and SCID mice were injected with ICG. The ICG concentrations in the mouse sera were subsequently monitored (**e**). The clearance rate of ICG was similar between the SCID and chimeric mice (**f**). The sinusoidal blood flow in the chimeric mouse liver was approximately one-half of that in the SCID mouse liver (**g**). The oxygen consumption of c-heps and m-heps was monitored (**h**). The oxygen consumption of c-heps was 1/4.5 lower than that of m-heps. $^*P<0.05$, $^{**}P<0.01$.